

# CHAPTER 5 - ANALYSIS OF RANDOM LEAK ARRIVALS

## 5.1 Introduction

As discussed in the previous chapters, the pinhole corrosion leak in home plumbing has emerged as a significant issue. In the major water distribution system managed by municipalities and water utilities the costs are distributed among all subscribers. However, the home plumbing repair/replacement cost and possible water damage cost must be addressed by the home owner. For most homeowners, the home is their most valuable asset. The possibility of falling home value, losing home insurance, water damage, frequent repairs, taste and odor, and health concerns are some key issues involved in home plumbing maintenance. The homeowner has to decide at the time of pinhole leak whether to repair or replace the system. If the owner decides to replace the system, another decision on which material to use should be made. Local regulations may not permit use of certain materials. In new homes, the plumbing contractor may decide the material.

The replacement decision depends on three factors: (1) financial affordability, (2) hydraulics of flow within the plumbing pipes, and (3) quality of water. Figure 5.1 shows the effect of financial viability. The accelerated replacement refers to replacing the plumbing system well in advance of the optimal replacement time. Delayed replacement ideally includes all the consequences of neglecting repairs or just performing repairs amounting to paying penalties to compensate for high replacement cost.

Hydraulics related to plumbing pipes addresses velocity, pressure and flow through numerous appurtenances along with temperature for hot water. The wall thickness of plumbing pipes rarely exceeds 2mm and diameter varies between 0.5 inches to 1 inch. The street level pressure of the major system is the key determinant in designing a plumbing system. If the pressure is high, it must be dissipated by frictional and minor losses with a maximum velocity range of 4-8 ft/sec (Nielsen, 1990). The velocity limitations are chosen to protect against

corrosion and cavitation and pressure rise due to stoppage of flow (water hammer). The time between leaks depends on the flow behavior but not well understood. From the Washington Suburban Sanitary Commission (WSSC) pinhole leak data (see chapter 4), it's found that leaks tend to cluster near treatment plants. High pressure and chlorine regions typically surround treatment plants and it's anticipated that high pressures and chlorine might play a role in pinhole leaks. It's also observed that if a corrosion pit is initiated due to high stress or water quality, velocity can aggravate and dominate pit growth.

Water quality poses two kinds of threats: initiation of corrosion and possible further degradation of quality from interaction with corroded elements. Copper reacts with oxygenated water to form a thin corroded layer of copper oxide which inhibits further corrosion and protects the metal underneath. If the water velocity is greater than 4 ft/sec, the oxide layer may be destroyed and the metal can corrode. (Taber, G. "corrosion in open and closed systems" PM engineer 2000; available at [http://www.pmengineer.com/CDA/ArticleInformation/features/BNP\\_Features\\_Item/0,2732,8783,00.html](http://www.pmengineer.com/CDA/ArticleInformation/features/BNP_Features_Item/0,2732,8783,00.html)). Taber (2000) cites amount of oxygen, chemicals present in water, presence of dissimilar metals, temperature, pressure, and flow rate to be the key factors in corrosion.

Rushing et al. (2004) report that the combination of pH greater than 8.2, aluminum deposits greater than 50 ppb and chlorine concentrate of 2 mg/l will result in copper pipe corrosion. A 90 degree bend in the pipe will accelerate corrosion due to this recipe. As shown in Figure 5.2, both hydraulic and water quality effects determine the nature of leak arrival times. In this thesis the net effect of these two causal phenomena in the form of the failure time data is considered. Unfortunately, the only available data is as shown in Figure 5.3, the leak rate data. The homeowner data is obtained from WSSC. It does not contain leak arrival times which are crucial in a decision model. In this chapter, we present a model that can yield leak arrival times from specified leak rates.

The repair/ replacement process is visualized as follows. The pinhole leaks arrive randomly. The leaks occur at random locations and at random time intervals. From a cost analysis point of view the random locations may not be that critical than the expenditure incurred. Therefore, at a broader level in minimizing the cost, the arrival times of pinhole leaks will dictate the repair/ replacement decision. It is also possible that the arrival of the first leak serves as a harbinger of subsequent, immediate leaks. However, present data suggest that such a uniform corrosion behavior is not evident. Another point of view is based on time; whether the leak occurs at an early stage of installation perhaps indicating installation flaws or occurring at a late stage indicating a deteriorating system; or within the anticipated normal design life. The early, normal, late stage of a plumbing system, possibility of clustering of leak occurrences in time, point to leak arrival patterns in time. The leak rate itself is a time dependent function. The rather high leak rates shown in Figure 5.3 suggest late stage behavior. In this chapter, several models that fit this late stage break rate are formulated. These models are used to infer the early and normal stage leak rate behavior.

A non-homogeneous poisson process (NHPP) model is considered for modeling the leak arrivals. This construct enables the development of a minimum cost model in terms of when the expenditures are incurred. The minimum cost model is based on the following notion. A risk-averse homeowner may decide to replace the plumbing system at a time well ahead of the optimal replacement called an accelerated replacement with the convenience of avoiding any major damages. It is not prudent to wait beyond the optimal replacement time called delayed replacement. Clearly, the advantage lies in exercising the replacement at the optimal time.

Such an optimal replacement time is dictated by the arrival pattern of the leaks. In the following section 5.2, a minimum cost model is adopted from Loganathan, Park, and Sherali (2002). In section 5.3, several models for the observed leak rate are fitted. From these models, the complete leak rate behavior is synthesized. It's pointed out that only a subset of these fitted models is suitable for a plumbing system. In section 5.4, the NHPP model is presented

in detail. Section 5.5 contains an example application that displays the variability in the leak arrival patterns.

## 5.2 Repair/Replacement analysis

At the time of the  $n^{\text{th}}$  leak, a decision has to be made whether to replace the plumbing system at a cost of  $F_n$  or to repair it at a cost of  $C_n$ . The scenario also implies that for the previous ( $n - 1$ ) leaks only repairs have been performed. If we assume that the plumbing will be replaced ( $C_n$  included in the sum should be adjusted for  $F_n$  when necessary) at the time of  $n^{\text{th}}$  leak,  $t_n$ , we can write the present worth of the total cost of the pipe as:

$$T_n = \sum_{i=1}^n \left( \frac{C_i}{(1+R)^{t_i}} + \frac{F_n}{(1+R)^{t_n}} \right) \quad (5-1)$$

in which:  $R$  = discount rate,  $t_i$  = time of  $i^{\text{th}}$  leak measured from the installation year (year),  $C_i$  = repair cost of  $i^{\text{th}}$  break,  $F_n$  = replacement cost at time,  $t_n$ ,  $T_n$  = total cost at time '0' (present worth).

When the system is new, it tends to experience very few leaks. An old system experiences more leaks under the same conditions. Therefore, the combination of varying time interval between leaks (accelerated leak arrivals towards the end), relatively smaller repair cost, and a generally large replacement cost leads to the existence of a "U" shaped present worth of the total cost curve over time (Figure 5.1).

The derivation of the threshold break rate seeks the time of the minimum present worth total cost. Loganathan et al. (2002) have presented the following threshold break rate ( $\text{Brk}_{\text{th}}$ ) equation

$$\text{Brk}_{\text{th}} > \frac{\ln(1+R)}{\ln\left(\frac{C_{n+1}}{F_n} + 1\right)} \quad (5-2)$$

in which:  $C_{n+1}$  = repair cost at  $(n+1)^{\text{th}}$  leak and  $F_n$  = replacement cost.

From the observed data for any given system we can derive a current leak rate. Whenever the

current leak rate,  $Brk_{cur}$  equals or exceeds  $Brk_{th}$  for the first time, the plumbing system should be replaced. Figure 5.3 shows the observed behavior for leak rate as a function of plumbing system installation period (WSSC data).

### 5.3 Leak rate models

#### 5.3.1 Shamir and Howard's model

Note that for the optimal replacement time, the earliest time at which Eq. (5-2) is satisfied must be chosen. From the optimal time onwards for any time,  $t$ , Eq. (5-2) will be satisfied. In order to infer the earliest time at which Eq. (5-2) holds it is necessary to generate leak arrival times. To mimic the actual occurrence of leaks, we adopt the following model due to Shamir and Howard (1979) given by

$$N(t) = N(t_0)e^{A(t-t_0)} \quad (5-3)$$

Where  $N(t)$  = number of leaks in year  $t$ ;  $t$  = time in years;  $t_0$  = base year for the analysis (pipe installation year, or the first year for which leak data are available); and  $A$  = growth rate coefficient (1/year).

#### Problem 1

Setting the leak rate  $N(t)$  to be equal to the  $Brk_{th}$  given in the previous section, we obtain the optimal time of replacement

$$t^* = t_0 + \frac{1}{A} \ln \left[ \frac{\ln(1+R)F_n}{N(t_0)C_{n+1}} \right] \quad (5-4)$$

For suitably chosen values of  $t^*$  of replacement time, initial values for  $N(t_0)$ ,  $A$ , and  $t_0$  can be obtained. From Eq. (5-4),  $t^*$  is assumed to be 25 and 35 years which could be optimal replacement times. The parameters  $R$ ,  $F_n$ ,  $C_{n+1}$ , and  $t_0$  are constants. For each  $t^*$  value, the  $N(t_0)$  and  $A$  can have different pairs of values.

Another procedure is to optimally select the parameters  $N(t_0)$ ,  $A$ , and  $t_0$  for a suitably chosen objective function. We choose to minimize the sum of the absolute deviations between the calculated and observed leak rates shown in Figure 5.3. That is,

**Problem 2**

Minimize  $\sum_t e_t^+ + e_t^-$

Subject to;  $At + b + e_t^- - e_t^+ = \ln [\text{observed break rate}]$  for all  $t$ .

where  $b = \ln [N(t_0)]$  and  $t_0 = 0$

$e_t^-$  and  $e_t^+$  or slack (convert less than or equal to type constraints into an equation) and surplus (convert greater than or equal to type constraints into an equation) variables

For non-negativity restrictions we write  $A = A^+ - A^-$ ,  $b = b^+ - b^-$ ,

and  $A^+, A^-, b^+, b^-, e_t^+, e_t^- \geq 0$

Problem P2 is a linear program. From the optimal values for  $N(t_0)$  and  $A$ , we can determine  $N(t)$  for any  $t$ .

In the WSSC data it's not clear when the plumbing systems were installed. Therefore, it was arbitrarily decided that the WSSC leak rates apply for houses that are 30 years and older.

When the on going survey from MUSES project in Virginia Tech is incorporated, more satisfactory results can be expected.

**5.3.2 Neural network model**

Our discussion on neural network modeling closely follows the discussion in Winston and Venkataramanan (2003). Consider Figure 5.4. Each square in Figure 5.4 is a cell of the network also called a neuron.

The first column of cells is the input layer and the cells are set at the input values. The network in Figure 5.4 is a feed forward network in the sense that the results go to only the higher layers; there are no feed back loops called “recurrent networks”. Cell 0 is called the bias that constitutes a constant input to the next layer. Cell 10 in the last column is the output cell and the last layer is the output layer. All other columns between the input and output columns are called the hidden layers. For any cell  $j$  not in the input layer, its input  $INP(j)$  is given by

$$INP(j) = \sum_i w_{ij} (\text{output from cell } i) \quad (5-5)$$

The output of  $j$  (not in the input layer) is obtained by the use of a transfer function  $f$ . the output of  $j$ ,  $OUT(j)$  is given as

$$OUT(j) = f[INP(j)] \quad (5-6)$$

The optimal weights  $w_{ij}$  are determined by minimizing the sum of squared differences between the calculated outputs at cell 10 (see Figure 5.4)  $OUT_k(10)$  and the corresponding observed values  $O_k(10)$  given by  $\sum_k [OUT_k(10) - O_k(10)]^2$  for the output layer. While the above description clearly parallels regression analysis, it is the ability to introduce hidden layers that enables neural networks to solve complicated problems. Also, standard functions such as the logistic sigmoidal function given by

$$f(a) = \frac{1}{1 + \exp(-a)} \quad (5-7)$$

and the *tan h* function given by

$$f(a) = \frac{e^a - e^{-a}}{e^a + e^{-a}} \quad (5-8)$$

are used as the transfer functions. In this chapter, the software PREDICT (produced by NEURALWARE) is used to fit the neural network model.

## **NeuralWorks PREDICT Software**

As mentioned above, neural networks are useful when an unknown relationship exists between a set of input data and output data. They can detect trends in data, generalize the data, and predict the outcome. To build a model with PREDICT software involves 3 steps: (1) collection of data and pre-processing, (2) building and training (to learn the structure of the data) the network, (3) testing and validating the network. Based on the input and the corresponding output provided, PREDICT automatically selects, trains, tests, and validates the model. A tutorial on using PREDICT is given in the Appendix B.

### **5.4 Simulation of leak occurrences**

In section 5.2, repair/replacement analysis Eq. (5-2) yields optimal replacement as the earliest time at which the condition is satisfied (i.e. satisfied for the first time). Unfortunately, the leak rates given in Figure 5.3 for the WSSC display a late stage behavior (bathtub curve is composed of early, stable, and late stage behavior). In section 5.3, we develop two types of leak rate models namely, an optimization model, Problem P2, and a neural network model. The purpose of these models is to provide an ability to backtrack through leak rate behavior to identify the potential early and normal stage leak rates. These two models provide leak rates throughout the life of a home plumbing system. Potentially, one can assess the leak rates at various times from these two models to use in Eq. (5-2). However, we find generating possible sequences of leak occurrence times has value in terms of ranges (descriptive statistics) for the leak times generated. Also, certain cost details such as total cost can be obtained. Moreover, it presents a comprehensive analysis of leak occurrence behavior.

#### **5.4.1 Non-homogeneous poisson process (NHPP)**

In the non-homogeneous poisson process, we permit the poisson parameter  $\lambda$  to be a function of time,  $\lambda(t)$ . Because leak rates vary with the age of the plumbing system, such a



model is necessary. The NHPP also known as non-stationary poisson process is given by (Law and Kelton, 2000).

$$P[ N( t+s ) - N(t) = k ] = \frac{e^{-b(t,s)} [b(t,s)]^k}{k!} \quad (5-9)$$

$$(for k=0,1,2,.. and t,s \geq 0, and b(t,s) = \theta(t+s) - \theta(t) = \int_t^{t+s} \lambda(y)dy)$$

in which  $\theta(t)$  is called the expectation function and  $\lambda(t)$  is the rate or intensity function.

Using the leak rate models developed in section 5.3 for  $\lambda(t)$ , we present the following procedure for generating the leak occurrence times.

#### 5.4.2 Simulation of Non-Homogeneous Poisson Processes (Thinning process)

1. Let  $\lambda = \max\{\lambda(t)\}$  be finite.
2. Generate a stationary Poisson process with constant rate  $\lambda$  and arrival times  $\{t_i\}$ . For the Poisson process with parameter  $\lambda$ , the inter-arrival times are exponentially distributed with parameter  $\lambda$ .

To generate exponentially distributed inter-arrival times randomly, we observe the following  $F(x) = 1 - e^{-\lambda x}$ . From uniform random number generator obtain  $U \sim U(0, 1)$  for  $F(x)$ .

For  $U = 1 - e^{-\lambda x}$ , we obtain  $X = -\frac{1}{\lambda} \ln(1-U)$ . Because  $(1-U) \sim U(0, 1)$ ,

we also have  $x = -\frac{1}{\lambda} \ln U$ . Because  $x$  represents the inter-arrival times only, we set

the arrival time  $t_i = t_{i-1} + x_i$  in which  $t_i$  is the arrival time of the  $i^{\text{th}}$  arrival and  $x_i$  is the inter-arrival time between the  $(i-1)^{\text{st}}$  and  $i^{\text{th}}$  arrivals.

3. Following Ross (1996), we make the following observation. Consider a homogeneous Poisson process with parameter  $\lambda$ , we count an event that occurs at time  $t$  from the homogeneous process with probability  $\frac{\lambda(t)}{\lambda}$ . The counted events then follow a non-homogeneous process with parameter  $\lambda(t)$ . Using

the above results, for each arrival time  $t_i$ , we generate a  $U_i \sim U(0, 1)$ . If  $U_i \leq \frac{\lambda(t_i)}{\lambda}$ , we consider the event at  $t_i$  as counted. Note we have  $t_i$  from step 2. More formally let

$$I_i = \begin{cases} 1 & \text{if } U_i \leq \frac{\lambda(t_i)}{\lambda} \\ 0 & \text{if otherwise} \end{cases}$$

Let the counted indices be denoted by the set  $J = \{i: I_i = 1\}$

The events at times  $t_i$  for  $i \in J$ , constitute the non-homogeneous Poisson arrivals.

Following Law and Kelton (2000), the above steps can be implemented as:

Assume that  $t_{i-1}$  has been validly generated and want to generate the next arrival time  $t_i$ :

1. Let  $t_0 = 0$ .
2. Set  $t = t_{i-1}$
3. Generate  $U_1$  and  $U_2$  as IID (Independent Identically Distributed)  $U(0,1)$  independent of any previous random variates.
4. Replace  $t$  by  $t - (1/\lambda) \ln U_1$ .
5. If  $U_2 \leq \lambda(t)/\lambda$ , return  $t_i = t$ . Otherwise, go back to step 2.

If the evaluation of  $\lambda(t)$  is slow, ( $\lambda(t)$  is a complicated function involving exponential and trigonometric calculations), computation time might be saved in step 4 by adding an acceptance pretest; i.e., the current value for  $t$  is automatically accepted as the next arrival time if  $U_2 \leq \lambda_* / \lambda$ , where  $\lambda_* = \min\{\lambda(t)\}$  and  $\lambda = \max\{\lambda(t)\}$ . This would be useful especially when  $\lambda(t)$  is fairly flat.

## 5.5 Application to WSSC data

The methodology described in this chapter is applied to the observed data from Washington Suburban Sanitary Commission (WSSC). The leak rates are shown in Figure 5.3. Unfortunately, it is not clear at what ages of a plumbing system the leak rates shown apply. Therefore, we have chosen to apply various lag periods starting at 30 years for the leak rate behavior. Assuming a design life of 50 years for copper plumbing systems, we assume lags of 30, 35... years would capture late stage deterioration behavior. Problem P2, optimization formulation in terms of WSSC data is given in Tables 5.1 and 5.2. The results along with the observed data are shown in Table 5.1. Clearly, the match is very good.

Next we apply the neural network methodology. Unfortunately with very few data points we cannot fit a neural network model. Therefore, we append data points arbitrarily that are very close to the observed data. These points are obtained by interpolation between the observed data. Linear optimization results along with these data are shown in Table 5.2. Using the expanded data set, we fit both the optimization model and the neural network model. The model results are shown in Figure 5.5. As the LP results shows, it is seen that 30 year lagged observed values and Shamir and Howard's graph match well. For the expanded data set, as the Shamir and Howard's equation is exponential, it fits earlier parts, but does not fit well the normal and late stages. On the contrary, neural network fit the data well. It's showing an S-shape curve and mimics all stages very well. Various curves are fitted in Figure 5.5 with the neural network model performing the best.

Possible leak scenarios are generated as shown in Table 5.3 using Table 5.4 neural network leak rates. In Table 5.3 the first, second, and third leak arrival times are 2, 8, and 16 years respectively. The thinning process is simulated 1,000 times and the mean, median, maximum, minimum, and standard deviation statistics for each leak arrival time are computed in Table 5.5. This is done with MATLAB and the source code is given in the Appendix C. For the rejection probabilities,  $\lambda(t)$  values are obtained from the neural network model as shown in

Table 5.4. The results of 1,000 simulations are summarized in Table 5.5. The distributions of leak arrival times are shown in Figure 5.6. From the shape of the distribution, each leak occurrence appears to fit a gamma distribution.

From the simulated possible leak scenarios, economic analysis is performed to obtain the

optimal replacement time. Following Loganathan et al. (2002),  $t_{n+1} - t_n < \frac{\ln(\frac{C_{n+1}}{F_n} + \frac{F_{n+1}}{F_n})}{\ln(1+R)}$  is

the time when replacement should be considered. For home plumbing system using the data from a Plumber Survey we set,  $C_{n+1}$  (repair cost) = \$500,  $F_n = F_{n+1} = \$ 3,500$ , and  $R = 0.065$ . Then the right hand side value is 2.12. This can be interpreted as, when the inter-arrival time becomes smaller than 2.12 year, the system should be replaced.

Using the mean arrival times given in Table 5.5, the replacement should take place after 4<sup>th</sup> leak. The modal value also agrees. For the fitted leak rate model this optimal year of replacement is about 23 years. This result is from the assumptions that the WSSC data follows late stage behavior and some data is appended for training the neural network.

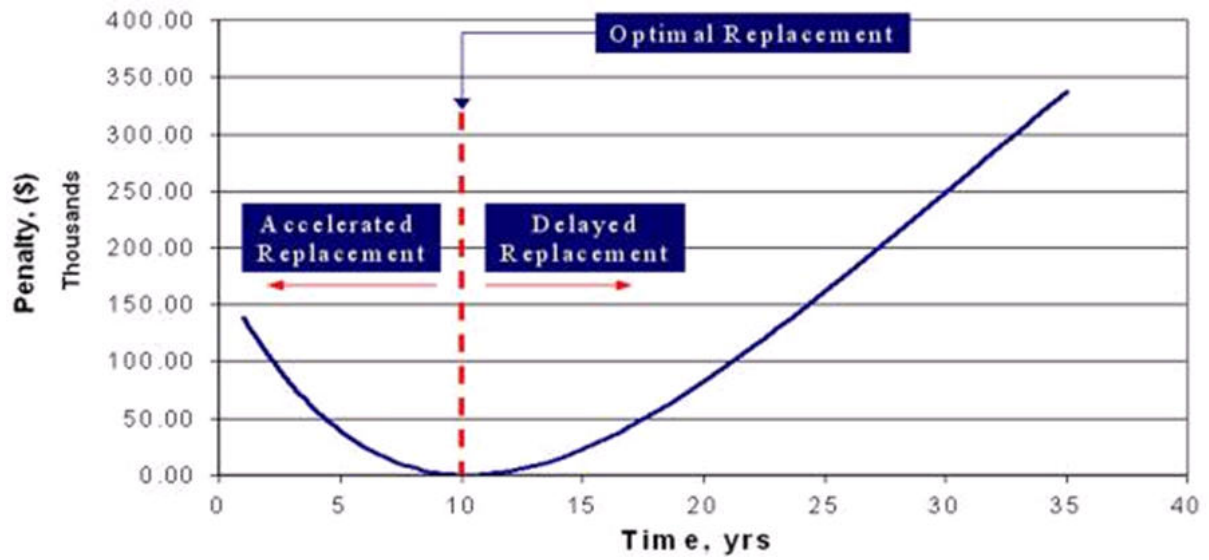


Figure 5.1 Plot of Present worth cost

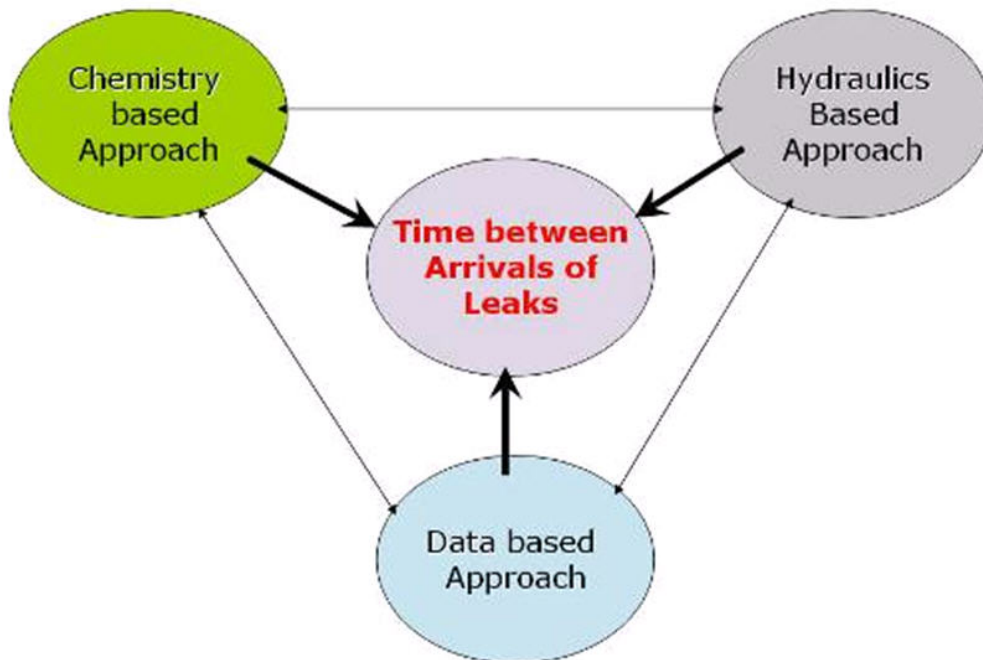


Figure 5.2 Hybrid methods

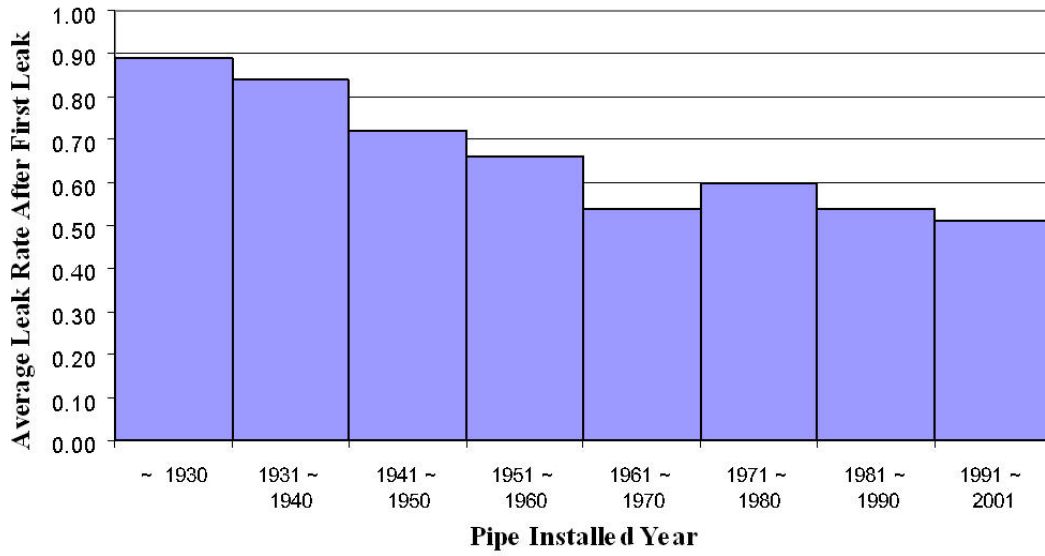


Figure 5.3 Observed leak rate

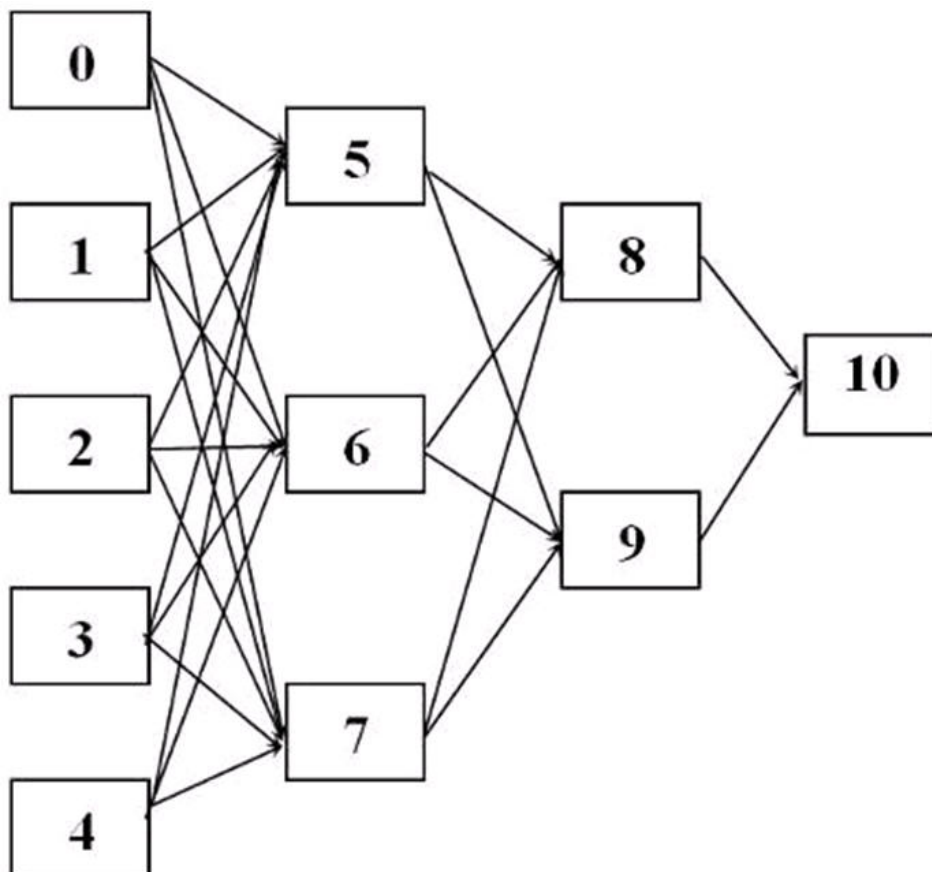


Figure 5.4 Feed forward back propagation neural network with two hidden layers

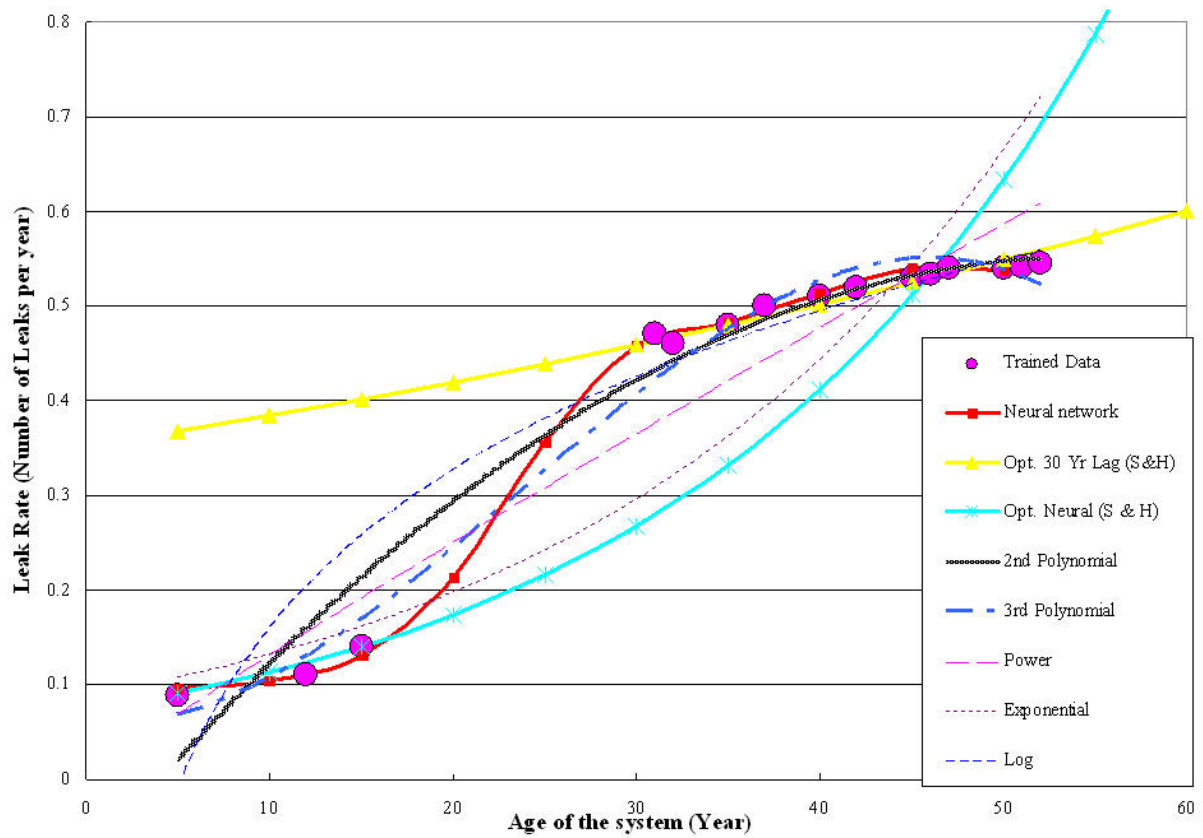
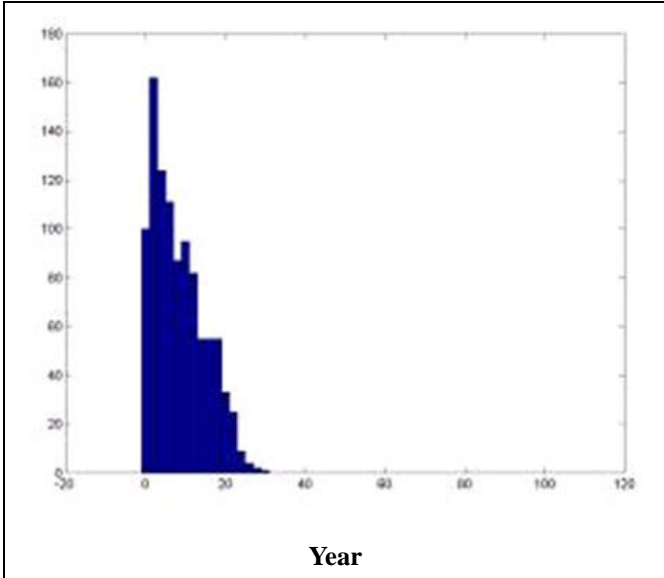
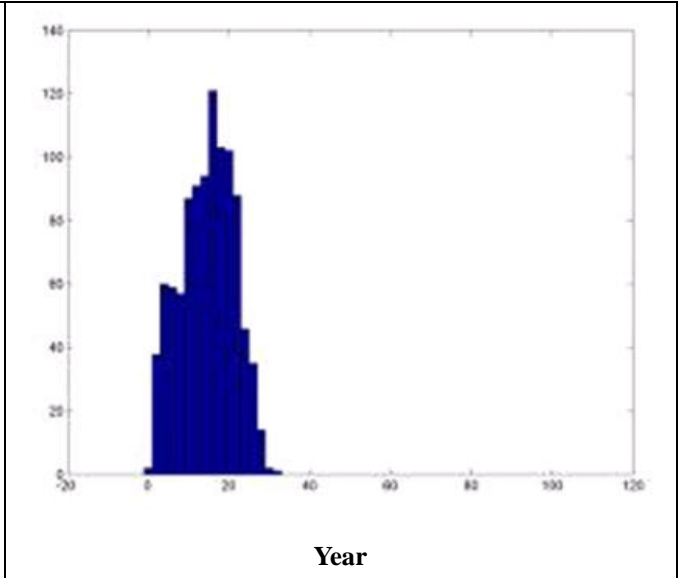


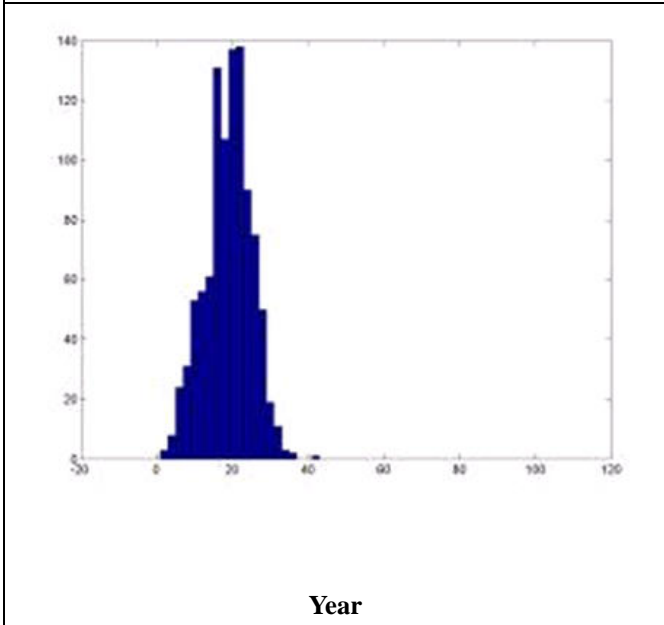
Figure 5.5 Prediction comparison



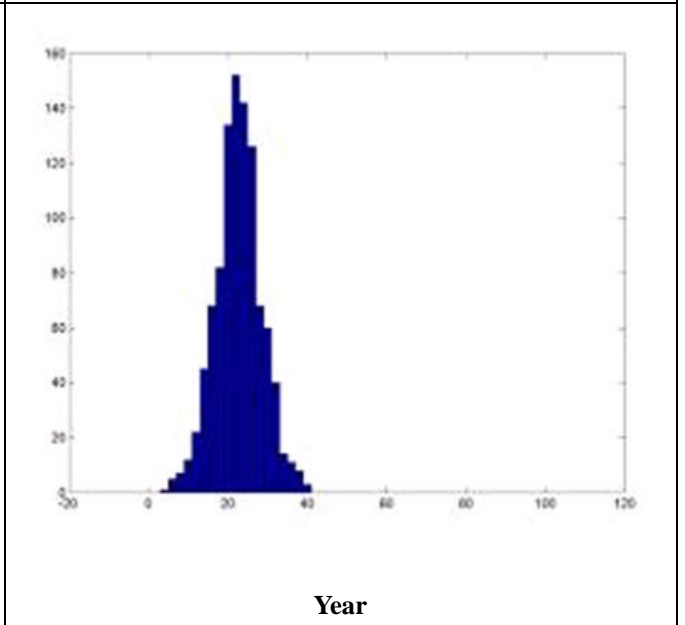
**1<sup>st</sup> Leak occurrence**



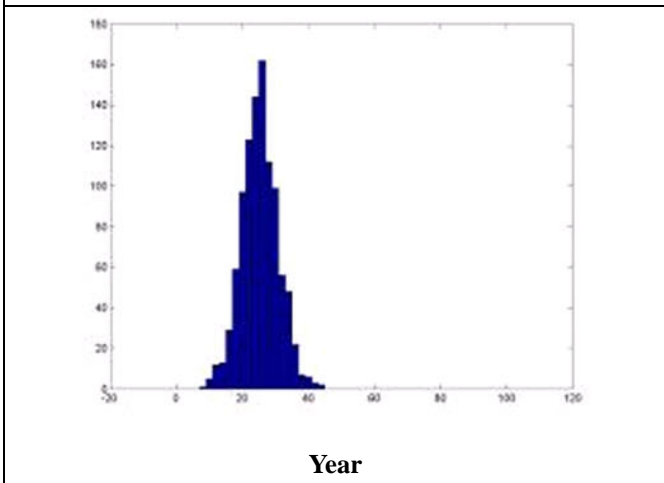
**2<sup>nd</sup> Leak occurrence**



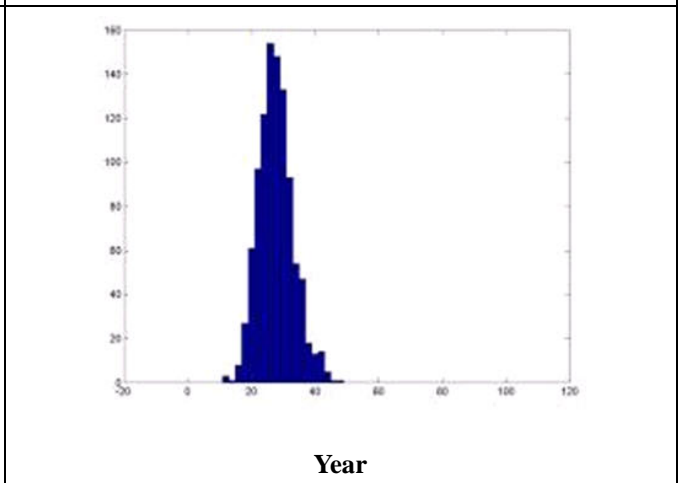
**3<sup>rd</sup> Leak occurrence**



**4<sup>th</sup> Leak occurrence**



**5<sup>th</sup> Leak occurrence**



**6<sup>th</sup> Leak occurrence**



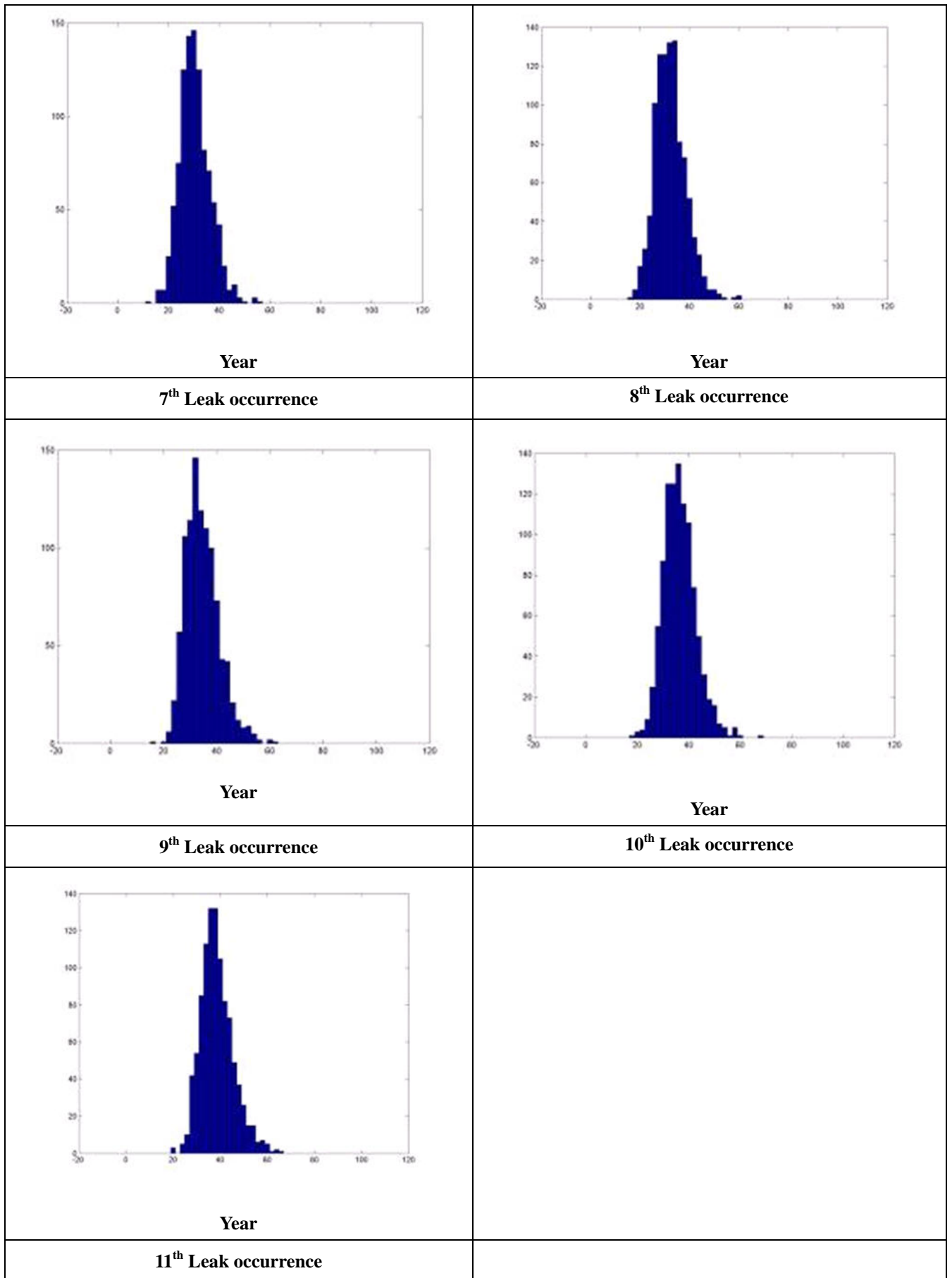


Figure 5.6 Distribution of leak occurrences

**Table 5.1 Results of Shamir- Howard Model (1979) (observed data only)**

Age of Plumbing System	Average Leak Rate	ln(Leak Rate)	Leak Rate calc		
35	<b>0.480</b>	-0.7340	<b>0.480</b>		
40	<b>0.510</b>	-0.6733	<b>0.502</b>		
45	<b>0.530</b>	-0.6349	<b>0.525</b>		
50	<b>0.540</b>	-0.6162	<b>0.549</b>		
55	<b>0.570</b>	-0.5621	<b>0.574</b>		
60	<b>0.600</b>	-0.5108	<b>0.600</b>		
65	<b>0.640</b>	-0.4463	<b>0.627</b>		
Ap	0.009	An	0.000	<b>A</b>	<b>0.00893</b>
bp	0.000	bn	1.046	<b>N(to)</b>	<b>0.35121</b>
C1p	0.000	C1n	0.000		
C2p	0.000	C2n	0.016		
C3p	0.000	C3n	0.010		
C4p	0.016	C4n	0.000		
C5p	0.007	C5n	0.000		
C6p	0.000	C6n	0.000		
C7p	0.000	C7n	0.020		
Con1	0.000		0.000		
Con2	0.000		-0.016		
Con3	0.000		-0.010		
Con4	0.000		0.016		
Con5	0.000		0.007		
Con6	0.000		0.000		
Con7	0.000		-0.020		
OBJ	0.069				

**Table 5.2 Results of Shamir-Howard Model (1979) (Modified data)**

Age of Plumbing System	Average Leak Rate	ln(Leak Rate)	Leak Rate calc		
5	<b>0.089</b>	-2.419	<b>0.091</b>		
12	<b>0.110</b>	-2.207	<b>0.123</b>		
15	<b>0.140</b>	-1.966	<b>0.140</b>		
31	<b>0.471</b>	-0.753	<b>0.279</b>		
32	<b>0.460</b>	-0.777	<b>0.292</b>		
35	<b>0.480</b>	-0.734	<b>0.332</b>		
37	<b>0.500</b>	-0.693	<b>0.362</b>		
40	<b>0.510</b>	-0.673	<b>0.412</b>		
42	<b>0.520</b>	-0.654	<b>0.449</b>		
45	<b>0.530</b>	-0.635	<b>0.511</b>		
46	<b>0.534</b>	-0.627	<b>0.534</b>		
47	<b>0.540</b>	-0.616	<b>0.558</b>		
50	<b>0.540</b>	-0.616	<b>0.635</b>		
51	<b>0.541</b>	-0.614	<b>0.663</b>		
52	<b>0.545</b>	-0.607	<b>0.692</b>		
Ap	0.04318559	An	0	<b>OBJ</b>	<b>2.83192</b>
bp	0	bn	2.61389677	<b>A</b>	<b>0.04319</b>
C1p	0.02115011	C1n	0	<b>N(to)</b>	<b>0.07325</b>
C2p	0.11160527	C2n	0		
C3p	0	C3n	0	Con1	-5E-16
C4p	0	C4n	0.52224617	Con2	-9E-16
C5p	0	C5n	0.45542897	Con3	-2E-16
C6p	0	C6n	0.3684318	Con4	-1E-15
C7p	0	C7n	0.32288261	Con5	-1E-15
C8p	0	C8n	0.21312845	Con6	-1E-15
C9p	0	C9n	0.14617535	Con7	-1E-15
C10p	0	C10n	0.03566676	Con8	-2E-15
C11p	0	C11n	0	Con9	-2E-15
C12p	0.03201229	C12n	0	Con10	-2E-15
C13p	0.16156908	C13n	0	Con11	-2E-15
C14p	0.20290453	C14n	0	Con12	-2E-15
C15p	0.23872361	C15n	0	Con13	-2E-15

				Con14	-2E-15
				Con15	-2E-15

**Table 5.3 Thinning procedure (1 iteration)**

U(0,1)	1-U(0,1)	HP_ exp-x	LeakTime	U(0,1)	LeakRate	lambda(t)/ lambda	NHPP
0.517	0.483	1.514	1.514	0.019	0.097	0.201	1.514
0.947	0.053	6.113	7.627	0.036	0.104	0.216	7.627
0.982	0.018	8.345	15.973	0.552	0.214	0.444	-999.000
0.213	0.787	0.499	16.472	0.079	0.214	0.444	16.472
0.045	0.955	0.095	16.567	0.204	0.214	0.444	16.567
0.646	0.354	2.164	18.731	0.587	0.214	0.444	-999.000
0.106	0.894	0.235	18.966	0.440	0.214	0.444	18.966
0.323	0.677	0.813	19.778	0.119	0.214	0.444	19.778
0.794	0.206	3.288	23.066	0.701	0.356	0.739	23.066
0.508	0.492	1.476	24.542	0.987	0.356	0.739	-999.000
0.852	0.148	3.977	28.520	0.265	0.458	0.950	28.520
0.011	0.989	0.023	28.542	0.921	0.458	0.950	28.542
0.710	0.290	2.580	31.123	0.111	0.482	1.000	31.123
0.659	0.341	2.243	33.366	0.521	0.482	1.000	33.366
0.707	0.293	2.555	35.921	0.987	0.483	1.002	35.921
0.423	0.577	1.145	37.067	0.462	0.483	1.002	37.067

**Table 5.4 Predicted leak rate from Neural Networks**

Age	Leak Rate
5	0.097
10	0.104
15	0.131
20	0.214
25	0.356
30	0.458
35	0.482

**Table 5.5 Possible leak scenario**

Leak Number	Mean (1)	Median (2)	Min (3)	Max (4)	Stdev (5)	Mode (6)
1 <sup>st</sup>	8.77	6.84	0.01	31.69	6.57	0
2 <sup>nd</sup>	15.08	14.91	0.52	35.41	6.67	15
3 <sup>rd</sup>	19.30	19.58	1.95	39.35	6.22	20
4 <sup>th</sup>	22.65	22.59	3.38	46.65	5.70	25
5 <sup>th</sup>	25.37	25.08	5.44	49.75	5.53	26
6 <sup>th</sup>	27.92	27.22	10.21	50.38	5.53	25
7 <sup>th</sup>	30.23	29.62	13.70	51.20	5.72	27
8 <sup>th</sup>	32.33	31.84	14.18	61.05	5.99	32
9 <sup>th</sup>	34.59	33.93	15.93	63.04	6.24	31
10 <sup>th</sup>	36.54	36.22	19.17	67.71	6.46	32
11 <sup>th</sup>	38.64	38.36	20.66	71.88	6.74	36
12 <sup>th</sup>	40.78	40.18	22.13	72.10	7.10	39